Pergamon

Int. J. Mach. Tools Manufact. Vol. 36, No. 8, pp. 925–937, 1996

0890-6955/96$15.00 + .00

0890-6955(96)00097-6

ADAPTIVE CUTTING FORCE CONTROL FOR A MACHINING CENTER BY USING INDIRECT CUTTING FORCE MEASUREMENTS

TAE-YONG KIM† and JONGWON KIM‡

(*Original received* 27 *June* 1995)

Abstract—This paper presents an adaptive cutting force controller for the milling process, which can be attached to most commercial CNC machining centers in a practical way. The cutting forces of x, y and z axes are measured indirectly from the use of currents drawn by a.c. feed-drive servo motors. A typical model for the feed-drive control system of a horizontal machining center is developed to analyze cutting force measurement from the drive motor. The pulsating milling forces can be measured indirectly within the bandwidth of the current feedback control loop of the feed-drive system. It is shown that indirectly measured cutting force signals can be used in the adaptive controller for cutting force regulation. The robust controller structure is adopted in the whole adaptive control scheme. The conditions under which the whole scheme is globally convergent and stable are presented. The suggested control scheme has been implemented into a commercial machining center, and a cutting experiment on face milling process is performed. Copyright © 1996 Elsevier Science Ltd

1. INTRODUCTION

During the past decades, the use of computer numerical control (CNC) machining centers has expanded rapidly. A great advantage of the CNC machining center is that it reduces the skill requirements of machine operators. However, the current CNC machining center necessitates the demand for qualified programmers. Since they have to develop CNC part programs off-line before the real machining stage, it is natural that they have a tendency to anticipate the worst machining conditions. Consequently, they select federates and spindle speeds which are unnecessarily low.

For this reason, most commercial CNC manufacturers provide an adaptive control function as optional equipment. The use of this function requires a set of upper and lower limits of the spindle motor currents, which have to be input into the CNC unit before the machining stage. During the cutting process, the CNC monitors the spindle current. If it goes beyond the upper limit, the CNC reduces the override of the programmed feedrate. If it goes under the lower limit, the CNC increases the override. In this way, the CNC tries to bound the spindle current within the given limits. However, this is not an adaptive control scheme in the control engineering sense and is rarely used in a flexible machining environment because there is so large a number of combinations of workpiece materials and tools.

On the other hand, in a laboratory environment, a series of studies on adaptive control with constraints (ACC) of cutting forces has been done. The state of the art is well reviewed by Ulsoy and Koren [1]. The basic objective is the on-line manipulation of the cutting conditions (typically feedrates) based on the measurement of actual cutting process characteristics (typically cutting forces). There have been many research activities in this area as done by Masory and Koren[2], Tomizuka *et al.* [3], Lauderbaugh and Ulsoy [4], Elbestawi *et al.* [5], etc.

However, as Ulsoy and Koren have mentioned, very few adaptive control systems have

†Engineering Research Center for Advanced Control and Instrumentation, Seoul National University san 56-1, Shinlim-Dong, Kwanak-Gu, Seoul, 151-742, Korea.

‡Department of Mechanical Design and Production Engineering, Seoul National University san 56-1, Shinlim-Dong, Kwanak-Gu, Seoul, 151-742, Korea.

been accepted by machine tool manufacturers so far since all the aforementioned research works have common practical drawbacks:

(1) Cutting force sensors, such as dynamometers, which are presently available, set many limits with respect to cost, wiring, reliability, and machine strokes.
(2) The controller structure should be more robust so that it can be applied reliably to various combinations of machining processes, workpiece materials and tools, without major changes of the control algorithm and parameters.

The objective of the research work reported in this paper is to develop an ACC system which can solve such practical drawbacks based on the following approaches:

(1) As a first point, in this research work, the cutting forces of x, y and z axes are measured indirectly from the use of currents drawn by feed-drive a.c. servo motors.
(2) Secondly, an adaptive robust servo control scheme for cutting force regulation is suggested, where the controller structure is a general pole assignment PID controller.

Stein *et al.* [6] studied the sensitivity analysis of the current drawn by d.c. servo drive motors to the cutting forces in turning processes. Altintas [7] discussed the viability of using armature current of a d.c. servo motor as a cutting force measurement sensor in milling processes. It has been verified that the pulsating milling forces can be predicted from the current measurement at tooth passing frequencies which are within the bandwidth of the servo. Since the contemporary CNC is adopting the a.c. servo-drive system, a new indirect cutting force measurement method should be studied on the a.c. servo-drive system, compared with the previous works on d.c. servo-drive systems.

The controller structure for cutting force regulation is another area to be studied further for practicality. Reviewing the previous studies on the controller structure for ACC systems shows a few works where adaptive control theory is applied to the cutting process control on a sound theoretical basis. The typical controller structure applied in these works is the implicit model reference adaptive controller (MRAC). It has been recognized, however, that a MRAC might result in oscillatory control signals if the open-loop zeros approach the instability region. This is because the MRAC controller works by pole-zero cancellation, which inherently limits robustness.

The remainder of this paper is organized as follows: in order to analyze the use of current signals from the a.c. feed-drive system for cutting force measurements, the modeling of the dynamic systems between cutting force signals and a.c. feed-drive current signals is presented in the next section. The subsequent section presents the controller structure which has been developed for robust adaptive cutting force regulation. The experimental results from the application of the suggested scheme to face cutting processes are shown. Finally, in the last section, the paper concludes with a short summary on the potential industrial application of the suggested system.

2. THE INDIRECT CUTTING FORCE SENSING SYSTEM

A horizontal machining center with a 32-bit microprocessor, FANUC CNC system model 15-M, has been used in this study. The three feed axes (x, y and z) of the machine have ball screw drives and are directly driven by permanent magnet synchronous (that is, PMSM type) a.c. servo motors. The servo motors are identical with each other, and the model number is FANUC A06B-0502-B. The model number of the servo-driver is FANUC T084/03-A20B-1003-008/02A. The block diagram of the feed-drive system can be derived as in Fig. 1 based upon the technical data provided from FANUC Ltd (Koga, [8]). There exists an inevitable time delay T at the input channel of the feedrate command when the command signal is processed at the programmable machine controller (PMC) of the CNC system.

The linear transfer function between the variation of the feedrate command v_c and the variation of the actual feedrate v_a for the x-axis feed-drive system is identified as

$$\frac{v_a(s)}{v_c(s)} = \frac{\omega_a(s)}{\omega_c(s)} = \frac{K_I K_{ip} K_t e^{-sT}}{J_e L_a s^3 + J_e(R_a + K_H K_{ip})s^2 + K_t(K_p K_{ip} + K_b)s + K_I K_t K_{ip}} \tag{1}$$

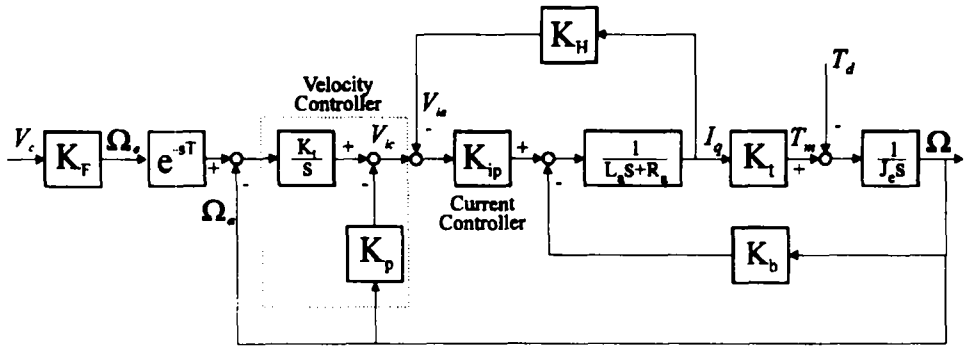

V_c	feedrate command [*mm* / min]	-	V_a	actual feedrate [*mm* / min]	-
Ω_c	ang. vel. command [*rad* / min]	-	Ω_a	actual ang. vel. [*rad* / min]	-
K_I	velocity integral gain [*V* / (*rad* / sec)]	8.2	K_F	ang. velocity gain [(*rad* / sec) / (*mm* / min)]	0.0105
K_p	velocity propotional gain [*V* / (*rad* / sec)]	0.4944	V_{ia}	feedback current [*V*]	-
V_{ic}	current command [*V*]	-	K_{ip}	current proportional gain [-]	7.5429
K_H	currnet feedback gain [*V* / *A*]	0.007	L_a	armature coil inductance [*mH*]	1.20
R_a	armature coil resistance [*ohms*]	0.15	I_q	actual current [*A*]	-
K_t	torque constant [*kgf* · *m* / *A*]	0.165	K_b	back EMF constant [*V* / (*rad* / sec)]	0.38
T_m	motor drive torque [*kgf* · *m*]	-	T_d	disturbance torque [*kgf* · *m*]	-
J_e	equivalent feed-drive inertia [*kgf* · *m* · sec^2]	0.0146	Ω	angular velocity of motor shaft [*rad* / sec]	-

Fig. 1. Block diagram of the FANUC feed-drive system.

Substituting the values given in Fig. 1 yields:

$$\frac{v_a(s)}{v_c(s)} = \frac{497000e^{-0.08s}}{(s + 14.0)(s^2 + 155s + 35500)} \tag{2}$$

Considering the practical frequency range of 0–10 Hz, the transfer function can be approximated by

$$\frac{v_a(s)}{v_c(s)} = \frac{14.0e^{-0.08s}}{s + 14.0} \tag{3}$$

Figure 2 shows a good agreement between the experimental and simulation step responses of the x-axis feed-drive system, which verifies the model presented in Fig. 1. The experimental and simulation frequency responses of the x-axis feed-drive system are shown in Fig. 3. The simulation response is in good agreement with the experimental result and the bandwidth of the velocity feedback control loop of the servo is about 2.3 Hz.

The dynamic characteristics of the current feedback control loop of the feed-drive system limit the bandwidth of the current sensing system for an indirect cutting force measurement. When the cutting force, that is the disturbance torque, is changing, if the current loop is not fast enough to compensate the current input into the servo motor, there should be an inherent limit to the indirect cutting force measurement system which predicts the cutting force from the current signals. This issue can be discussed in detail as follows.

In the model shown in Fig. 1, the motor drive torque T_m is exerted in accelerating the equivalent feed-drive inertia J_e, and in overcoming the disturbance torque T_d. The disturbance torque T_d consists of the friction torque in the drive T_f and the cutting torque T_c reflected on the motor shaft.

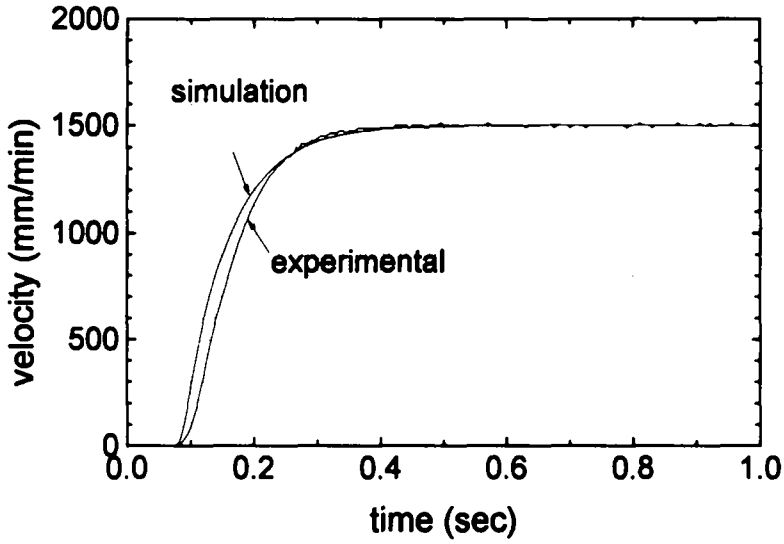

Fig. 2. Experimental and simulation step reponse of the x-axis feed-drive system.

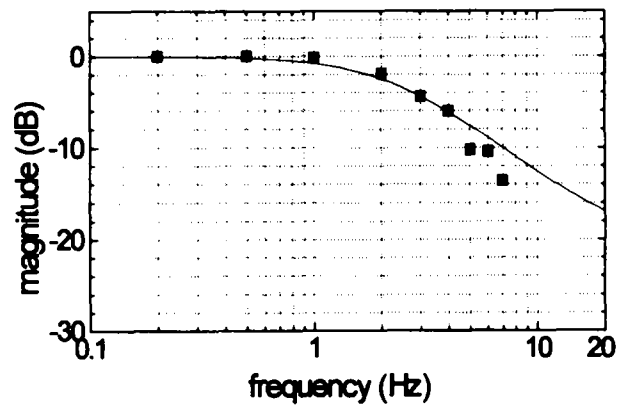

(a) magnitude

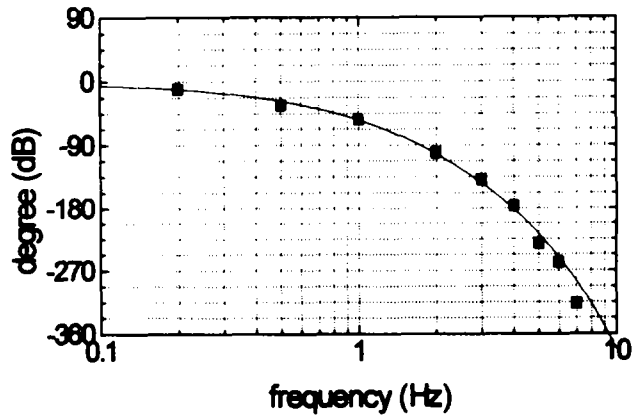

(b) phase

Fig. 3. Experimental and simulation frequency response of the x-axis feed-drive system $v_a(s)/v_c(s)$.

$$T_m = J_e \frac{d\Omega}{dt} + T_d \tag{4}$$

where

$$T_d = \text{sgn}(\Omega) T_f + T_c \tag{5}$$

On the other hand, the motor drive torque T_m is proportional to the current input to the servo motor. In the case of PMSM type a.c. servo motors, the following stator currents are controlled in phase:

$$\begin{aligned} I_u &= I_m \cos\theta_e \\ I_v &= I_m s \cos\left(\theta_e + \frac{2\pi}{3}\right) \\ I_w &= I_m \cos\left(\theta_e - \frac{2\pi}{3}\right) \end{aligned} \tag{6}$$

I_m is the amplitude of the stator current and Θ_e is the electrical angle of the phase current. The u- and v-phase stator currents, I_u and I_v, respectively can be measured with Hall sensors. The w-phase stator current can be calculated from the following relationship:

$$I_u + I_v + I_w = 0 \tag{7}$$

The relative angular position of the q-axis of the rotor Θ_m from the u-phase stator should be measured to calculate the motor drive torque T_m as follows:

$$T_m = K_t I_q \tag{8}$$

with

$$\begin{bmatrix} I_d \\ I_q \end{bmatrix} = \sqrt{\frac{2}{3}} \begin{bmatrix} \sin(\theta_e) & \sin\left(\theta_e + \frac{2}{3\pi}\right) & \sin\left(\theta_e - \frac{2}{3\pi}\right) \\ \cos(\theta_e) & \cos\left(\theta_e + \frac{2}{3\pi}\right) & \cos\left(\theta_e - \frac{2}{3\pi}\right) \end{bmatrix} \begin{bmatrix} I_u \\ I_v \\ I_w \end{bmatrix} \tag{9}$$

and

$$\theta_e = n_p \theta_m \tag{10}$$

K_t is a torque constant, I_d and I_q are the d and q-axis equivalent stator currents, respectively, and n_p is the number of magnetic poles. I_d is maintained at zero for the PMSM type a.c. servo motor.

From equation (4) and equation (8), assuming steady-state feedrates yields

$$K_t I_q = T_d = \text{sgn}(\Omega) T_f + K_f \tag{11}$$

where K_f is the cutting force transmission gain as a torque. A series of experimental cutting results in the following linear relationships from the least square regression of the recorded data of cutting forces F_c and equivalent currents I_q (see Fig. 4),

$$x\text{-axis: } I_{qx} = 4.12 + 0.00362 F_{cx} \tag{12}$$

$$y\text{-axis: } I_{qy} = 7.24 + 0.00450 F_{cy} \tag{13}$$

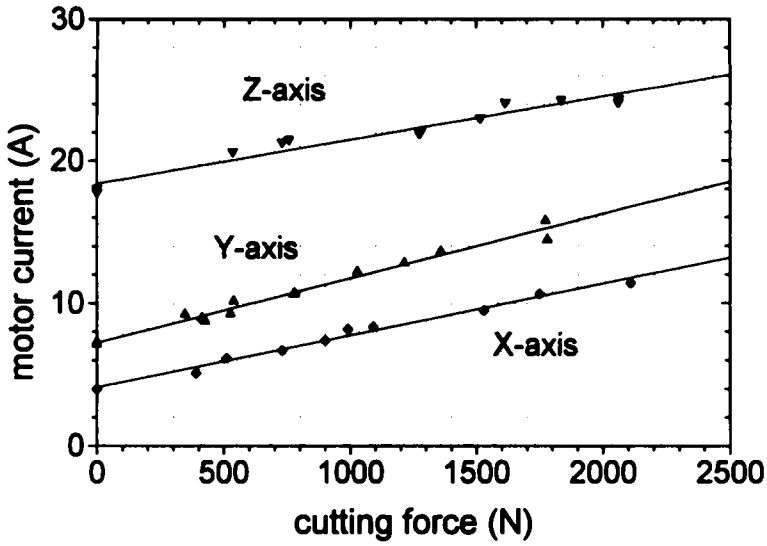

Fig. 4. Static characters of the indirect cutting force measurement system.

$$z\text{-axis: } I_{qx} = 18.5 + 0.00289F_{cx} \tag{14}$$

Equation (12), equation (13) and equation (14) describe the static characteristics of the indirect cutting force measurement system. The linear transfer function between i_q, which is the variation of the equivalent current I_q, and f_c, which is the variation of the cutting force F_c, for the x-axis feed-drive system, can be obtained from the block diagram shown in Fig. 1:

$$\frac{K_t i_q(s)}{t_d(s)} = \frac{3570(s + 139)}{(s + 14.0)(s^2 + 155s + 35500)} \tag{15}$$

where t_d is the variation of the disturbance torque T_d (see Fig. 1). This transfer function can be approximated as follows by neglecting the poles which do not strongly affect the current loop dynamics:

$$\frac{K_t i_q(s)}{K_f f_c(s)} = \frac{255(s + 139)}{s^2 + 155s + 35500} \tag{16}$$

The experimental and simulation frequency responses of the current-cutting force sensing system for the x-axis feed-drive system are shown in Fig. 5. The simulation response is in good agreement with the experimental results within the bandwidth of the system. The frequency response in Fig. 5 indicates that the current sensor bandwidth is approximately 62 Hz, and the cutting forces may be tracked by the current when tooth passing frequencies are below this frequency.

In Fig. 6, the measured cutting force and the current drawn from the servo motor are illustrated. The cutting force was measured by a Kistler table dynamometer. The cutting conditions are given in Fig. 6. The tooth passing frequency is 20 Hz. The current is in good agreement with the dynamometer force with a maximum deviation of about 100 N, which is within 8% of the steady-state error bound.

3. ROBUST ADAPTIVE CONTROL SCHEME FOR CUTTING FORCE REGULATION

An adaptive robust servo control scheme, combining on-line cutting process estimation and control, has been suggested by the authors [9]. The basic structure of the proposed adaptive controller consists of: (1) a controlled plant model; (2) a model parameter estimator; (3) a robust servo controller; and (4) a controller adjustment mechanism.

The controlled plant consists of a CNC feed-drive servo mechanism S and a cutting process

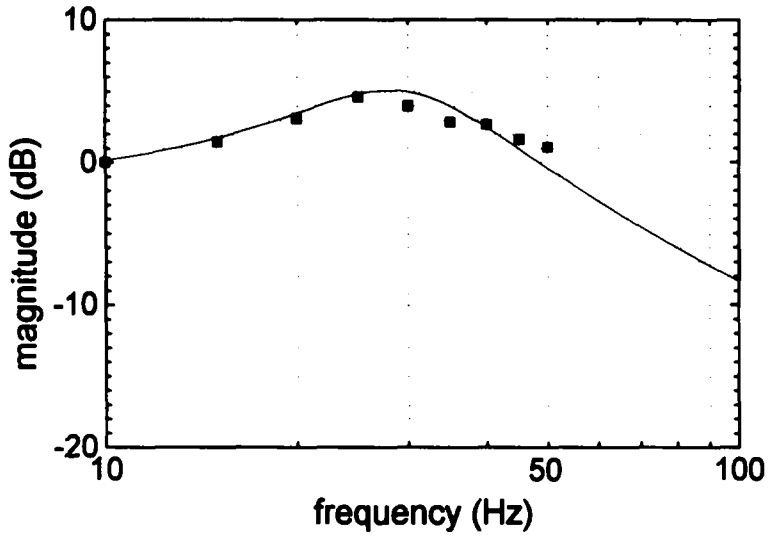

Fig. 5. Experimental and simulation frequency response of the current-cutting force system for the x-axis feed drive system, $K_t\, i_q(s)/K_f f_c(s)$.

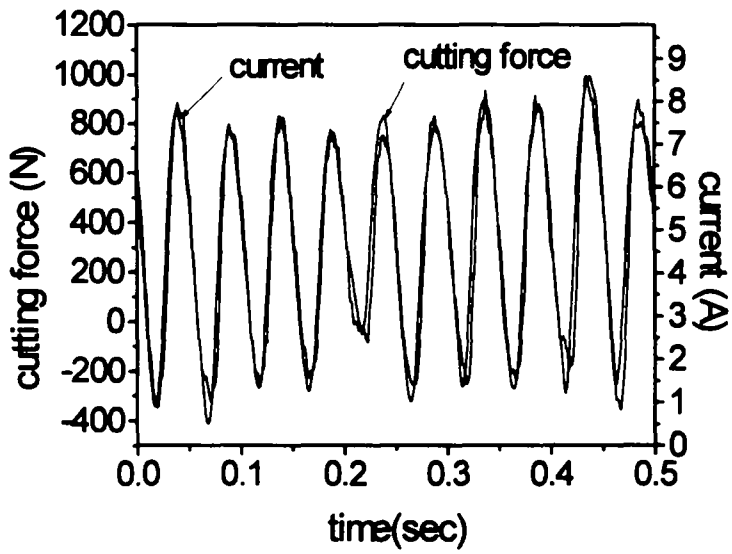

Fig. 6. Measured cutting force and the current from the x-axis servo motor (axial depth-of-cut 4 mm, radial depth-of-cut 20 mm, spindle speed 600 rpm, feedrate 300 mm min^{-1}, two flute end mill with dia. 20 mm).

P, as shown in Fig. 7. The control objective is to generate a series of feedrate command signals v_c which regulate the cutting force F_c so that its peak outputs maintain a constant allowable value regardless of the variation of depth-of-cut D and/or workpiece material M. The following discrete-time ARMA model is assumed for the controlled plant:

$$f_c(t) + \phi_1 f_c(t-1) + \phi_2 f_c(t-2) = \theta_0 v_c(t-1) + \theta_1 v_c(t-2) \tag{17}$$

where f_c (t) and v_c (t) are the sampled data series.

The controlled plant model equation (17) can be put into a block observable canonical form by defining a set of state vectors as follows:

$$\begin{cases} x_1(t-1) + \; -\phi_2 f_c(t-1) + \theta_1 v_c(t-1) \\ x_2(t) = x_1(t-1) - \phi_1 f_c(t-1) + \theta_0 v_c(t-1) \end{cases} \tag{18}$$

It can be written more compactly as:

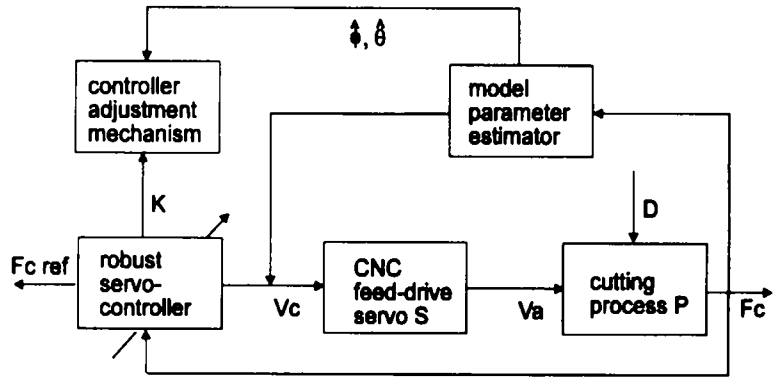

Fig. 7. Basic structure of an adaptive robust servo control for cutting force regulation.

$$\begin{cases} x(t+1) = \phi x(t) + \Gamma v_c(t) \\ f_c(t) = C_m x(t) \end{cases} \tag{19}$$

where

$$\begin{aligned} x(t) &\equiv [x_1(t), x_2(t)]' \\ \phi &\equiv \begin{bmatrix} 0 & -\phi_2 \\ 1 & -\phi_1 \end{bmatrix}; \Gamma = \begin{bmatrix} \theta_1 \\ \theta_0 \end{bmatrix} \\ C_m &= [0\ 1] \end{aligned} \tag{20}$$

Model equation (17) can be written in the following form:

$$f_c(t) = \phi_m(t-1)^T \theta_p \tag{21}$$

The model parameter vector θ_p is then estimated by using the on-line least squares method with covariance resetting and dead-zone control [10].

For the purpose of improving the robustness of the adaptive control scheme, achieving the explicit closed-pole assignment, and easily extending the whole scheme to multi-input multi-output cases, a robust servo controller structure is adopted, which consists of a servo compensator, a stabilizing compensator, and a feedback controller [11].

The servo compensator is constructed in such a way that its dynamic modes should be identical with those of command inputs and/or disturbances. This is a generalization of the integral controller of the classical control theory. Since the command input is a constant allowable cutting force in this research work, the servo compensator can be presented as follows:

$$\eta(t+1) = \eta(t) + Te(t); e(t) = f_c(t) - f^*_c(t) \tag{22}$$

where T is the sampling time (s) and f_c^* is the cutting force command input (N).

The stabilizing compensator stabilizes the augmented system which can be obtained by applying a servo compensator equation (22) to the controlled plant equation (19). A stabilizing compensator has been chosen:

$$\varepsilon(t+1) = \gamma_0 \varepsilon(t) + \gamma_1 f_c(t) + \gamma_2 \eta(t) \tag{23}$$

Applying the feedback controller

$$v_c(t) = k\eta(t) + \gamma_3 f_c(t) + \gamma_4 \varepsilon(t) \tag{24}$$

to the controlled plant equation (19) with the servo compensator equation (22) and the stabilizing compensator equation (23) yields the following closed-loop system:

$$X(t+1) \equiv \phi(\mathbf{K})X(t) + (\mathbf{K})f^*_c(t) \tag{25}$$

$$f_c(t) = C(\mathbf{K})X(t) \tag{26}$$

where

$$X(t) \equiv [x(t),\eta(t),\varepsilon(t)]' \in R^M \tag{27}$$

$$\phi(k) \equiv \begin{bmatrix} \phi + \Gamma\gamma_3 C_m & \Gamma k & \Gamma\gamma_4 \\ B^*_d C_m & C^*_d & 0 \\ \gamma_1 C_m & \gamma_2 & \gamma_0 \end{bmatrix} \tag{28}$$

$$\Gamma(\mathbf{K}) \equiv \begin{bmatrix} 0 \\ -B^*_d \\ 0 \end{bmatrix}; \; C(\mathbf{K}) = [C_m\ 0\ 0]^T \tag{29}$$

with $M = 4$ and $\mathbf{K}$ denoting the controller gain vector:

$$\mathbf{K} = [k,\gamma_0,\gamma_1,\gamma_2,\gamma_3,\gamma_4] \tag{30}$$

The closed-loop system equation (25) has following properties: there always exists $\mathbf{K}$ which can achieve zero tracking or regulation error with an arbitrary damping factor, and this controller is robust if and only if:

(1) the perturbations of the controlled plant model parameters do not make Φ unstable, and Φ is always asymptotically stable;
(2) (Φ, Γ) is controllable and (C_m, Φ) is observable;
(3) the number of measured outputs is greater than or equal to that of regulated outputs;
(4) the transmission zeroes of (C_m, Φ, Γ) do not coincide with the dynamic modes of the command inputs and disturbances; and
(5) the regulated output is physically measurable.

The controller gain vector $\mathbf{K}$ should be adjusted on-line so that the eigenvalues of $\Phi(\mathbf{K})$ of the closed loop system are assigned to the values which can produce a desired damping factor as well as asymptotic stability. In this research work, a parametric eigenstructure assignment approach by output feedback control [12] has been used for the desired closed-loop pole placement. This algorithm takes about 20 ms to calculate a new set of control gains $\mathbf{K}$ for a fourth order closed-loop system by using a personal computer (PC486 class with a clock speed of 66 MHz).

4. EXPERIMENTAL STUDIES

The schematic diagram of the entire experimental set-up is shown in Fig. 8. The base machine tool is a horizontal machining center, model MCH-10, designed and manufactured by Seil Heavy Industries in Korea. Attaching a current sensor to each of the u- and v-phase power cables of the x, y and z axis AC servo motors serves as the cutting force measurement method suggested in this paper. No additional dynamometer is needed. The u- and v-phase currents are fed back into an analog filter and an AD converter of a signal processing board in the PC486. The signal processing board also has a counter unit to monitor the encoder signals from the servo motors, which present the angular positions of the servo motor rotors. The adaptive control algorithm is implemented on the PC486. The current signals are collected at 500 Hz sampling frequency. The sampling frequency of the adaptive control algorithm is synchronized with the spindle spinning speed. It generates a new feedrate command input on each spin of the spindle.

The feedrate commands are transferred in a practical way to the CNC unit. The adaptive controller generates feedrate override signals ranging from zero to 255% of the programmed

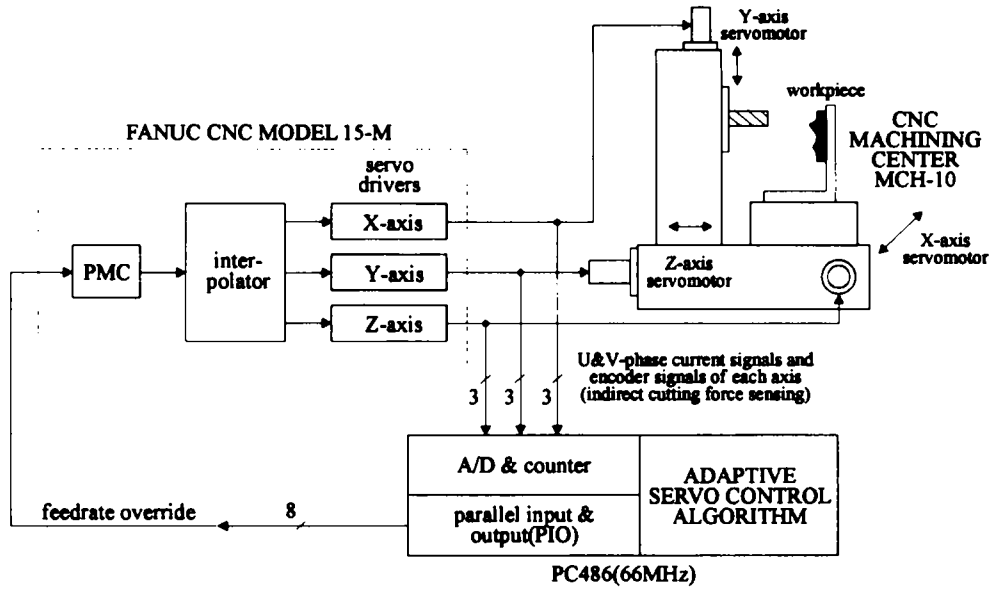

Fig. 8. Schematic diagram of the experimental setup.

feedrate and converts them into eight-bit binary signals. The parallel input/output (PIO) module of the signal processing board in the PC486 then transmits these binary signals to the programmable machine control (PMC) unit which is built into the CNC system. By using such an easily accessible interfacing method for cutting force sensing and feedrate command transmission, the developed ACC system can be added to most of commercial CNC machining centers as optional equipment.

The experimental study has been performed to show how the suggested ACC system works. The schematics of the experiment is shown in Fig. 9(a). The material of the workpiece on the right side is 1054 steel, and on the left side is aluminum alloy. The test cut starts from the right side to the left in the x-axis direction of the horizontal machining center. The spindle spinning speed is 400 rpm, and the tool is a three-inserts face-milling cutter with a diameter of 100 mm. The tooth passing frequency is 20 Hz. The radial depth-of-cut is 80 mm and the axial depth-of-cut is varied as shown in Fig. 9(b). The cutting force to be regulated is set to be 500 N in this case.

The control algorithm estimates a new set of model parameters and generates a new feedrate command input at each sampling interval. The sampling time of the on-line adaptive control is 100 ms, corresponding to one sample per spindle spin. The desired poles are assigned to z = 0.3, 0.35, 0.7 and 0.75 in the z-plane, which means that the desired damping coefficient is 1.0 and that the dominant natural frequency is 2.8 rad s^{-1}.

The results of real time cutting experiments are shown in Fig. 10. The controlled cutting force is the maximum amplitude per spindle revolution. The error bound of the controlled cutting force is within 50 N at the steady-state region for the desired command input of 500 N, regardless of the change of depth-of-cut and workpiece material [see Fig. 10(a)].

The feedrates are consequently changed from 360 mm min^{-1} for 1.0 mm depth-of-cut to 120 mm min^{-1} for 2.0 mm [see Fig. 10(b)]. At the second step change, the workpiece material is changed from 1054 steel to aluminum alloy. The depth-of-cut is maintained at 2.0 mm. The ACC system yields the same control performance through the adaptation algorithm. The feedrate increases from 120 to 320 mm min^{-1} even if the depth-of-cut is not changed. In this way, the feedrate can be selected on-line at the machining stage so that the productivity of the rough milling processes can be improved.

An overshoot occurs at every step change of depth-of-cut or workpiece materials. This is inevitable because the ACC system needs a certain amount of adaptation time to reach a new state. Fig. 10(c) shows that the model parameter estimates of the cutting process converge to

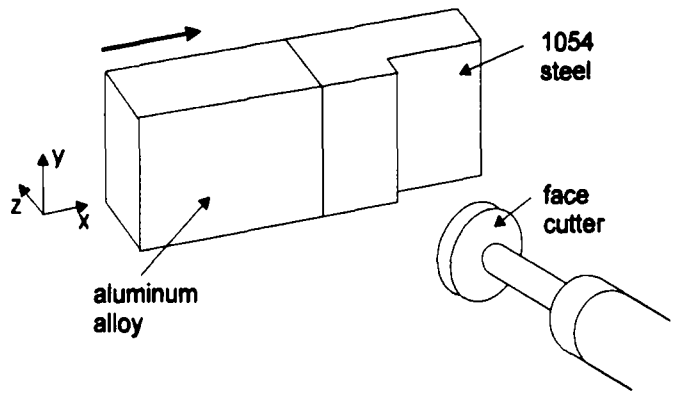

(a) Schematics

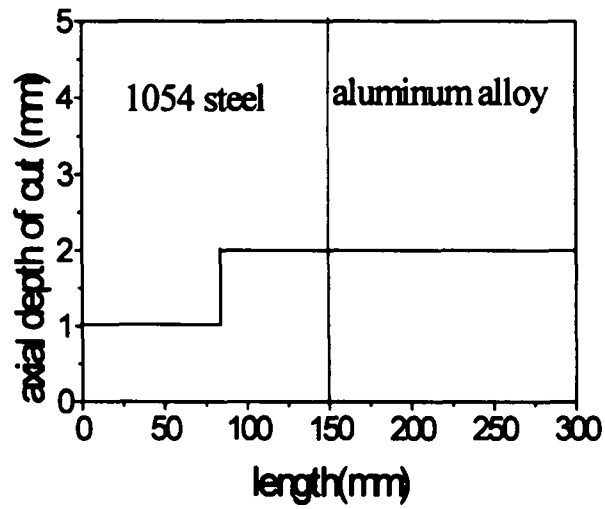

(b) Axial depth-of-cut

Fig. 9. Schematics of the experiment on the face cutting process.

a different set of steady-state constant values. The control gains are then updated for the new set of model parameters as shown in Fig. 10(d).

5. CONCLUSION

A research work on an indirect measurement of cutting forces for commercial machining centers and its application to the control of the cutting force has been presented. Since the recent CNC machine tools are equipped with a.c. servo drive systems, a new method to use the currents of a.c. servo drives has been developed. With the indirect cutting force measurement system, a practical ACC system for industrial application has been developed. In summary, the following conclusions can be drawn from this work:

(1) An indirect cutting force measuring system by using a.c. servo drive current sensing is developed without using a tool dynamometer. The static accuracy is within 8%, and the bandwidth is approximately 62 Hz. The dynamic characteristic of the current feedback control loop of the feed-drive system limits the bandwidth of the current sensing system for an indirect cutting force measurement.
(2) An adaptive robust servo control scheme for cutting force regulation is suggested, where

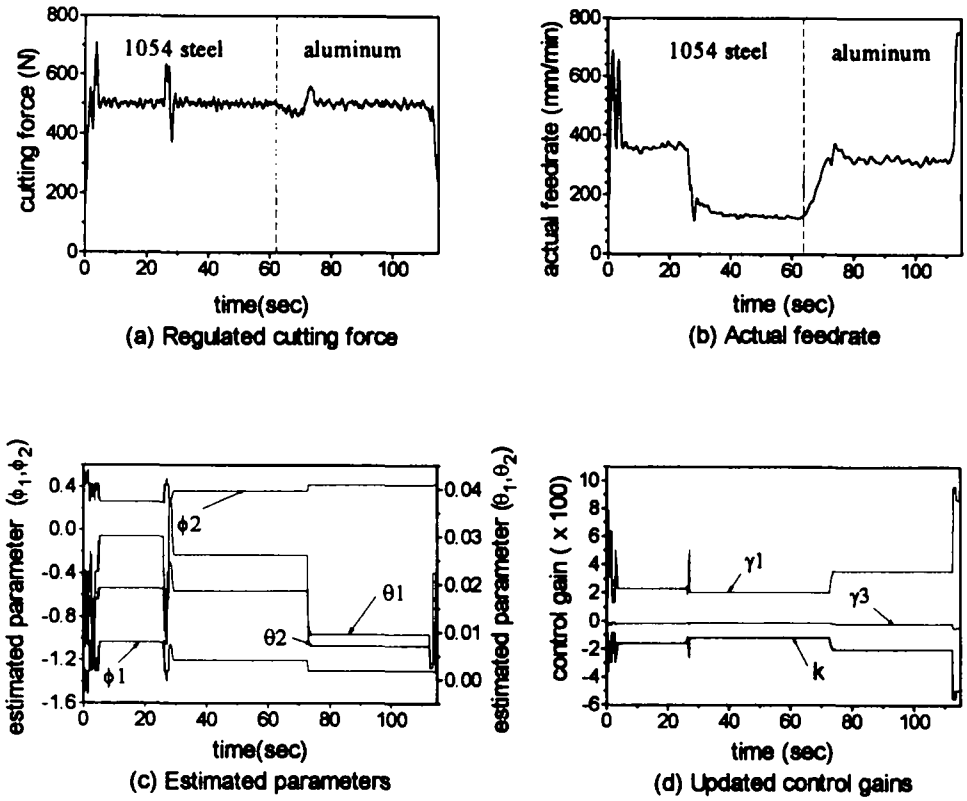

Fig. 10. Results of the real cutting experiment on the face cutting (spindle speed 400 rpm, three-tooth face cutter with dia. 100 mm, radial depth-of-cut 80 mm).

the controller structure is of a general pole assignment PID type. Arbitrary explicit pole assignment is possible.

(3) The real-time cutting experiment on face cutting processes reveals a good regulating performance of the suggested adaptive control scheme.

(4) Since the experimental set-up is implemented based on a commercial machining center through a standard interfacing method, the developed algorithm can be easily embedded into other machines as an optional equipment.

Acknowledgements—This work has been supported partly by the Engineering Research Center for Advanced Control and Instrumentation (ERC-ACI) at Seoul National University in Korea. The authors gratefully acknowledge the support.

REFERENCES

[1] A. G. Ulsoy and Y. Koren, Control of machining processes, *ASME J. Dyn. Systems Mesmt Cont.* **115,** 301–308 (1993).

[2] O. Masory and Y. Koren, Variable-gain adaptive control systems for machine tools, *J. Manufact. Systems* **2,** 165–174 (1983).

[3] N. Tomizuka, J. H. Oh and D. A. Dornfeld, Model reference adaptive control of the milling process, *Control of Manufacturing Processes and Robotic Systems, ASME Winter Annual Meeting*, November, New York, pp. 55–63 (1983).

[4] L. K. Lauderbaugh and A. G. Ulsoy, Model reference adaptive force control in milling, *ASME J. Engng Ind.* **111,** 13–21 (1989).

[5] M.A. Elbestawi, Y. Mohamed and L. Liu, Application of some parameter adaptive control algorithms in machining, *ASME J. Dyn. Systems Mesmt Cont.* **112,** 611–617 (1990).

[6] J.L. Stein, D. Colvin, G. Clever and C.H. Wang, Evaluation of DC servo machine tool feed drives as force sensors, *ASME J. Dyn. Systems Mesmt Cont.* **108,** 279–288 (1986).

[7] Y. Altintas, Prediction of cutting forces and tool breakage in milling from feed drive current measurements, *ASME J. Engng Ind.* **114,** 386–392 (1992).

[8] T. Koga, About the FANUC Digital Servo, a corresponding letter on the structure of the FANUC servo controller with the authors (1994).

[9] J. Kim and T. Y. Kim, Cutting force regulation by using an adaptive servo controller, *Proc. First S.M. Wu Memorial Symp.*, Northwestern University, pp. 379–386 (1994).

[10] G. C. Goodwin and K. S. Sin, *Adaptive Filtering, Prediction and Control.* Prentice-Hall, Englewood Cliffs, NJ (1984).
[11] E. J. Davison and I. J. Ferguson, The design of controllers for the multivariable robust servo mechanism problem using parameter optimization methods, *IEEE Trans. Autom. Cont.* **26**, 93–110 (1981).
[12] M. M. Fahmy and O'Reilly, Multistage Parametric eigenstructure assignment by output-feedback control, *Int. J. Cont.* **48**, 97–116 (1988).